

Scale effects and full-scale ship hydrodynamics: a review

Momchil Terziev^{1,*}, Tahsin Tezdogan², Atilla Incecik¹

¹ Faculty of Engineering, university of Strathclyde, Glasgow, UK

² Department of Naval Architecture, Ocean and Marine Engineering, University of Strathclyde, Glasgow, UK

*Corresponding author email: momchil.terziev@strath.ac.uk

Abstract

Historically, the field of naval architecture has relied on a combination of model testing and scaling laws, known as extrapolation procedures, to predict full-scale power requirements. Numerous problems with extrapolation procedures were identified almost as soon as they were proposed, but since there were no alternative scaling laws their use persisted. This review article explores the cause of these uncertainties, the attempts to circumvent or correct them, and the current efforts to reduce and even eliminate the need for extrapolation of ship resistance through the use of full-scale Computational Fluid Dynamics. We find that while there are a number of developments and accomplishments in achieving robust and reliable full-scale numerical simulation, the research community is not yet ready to replace experimentation and extrapolation. The principal bottlenecks are the availability of open full-scale data, including ship geometries, and computational power to predict full-scale flows with the necessary accuracy.

Keywords: *Ship hydrodynamics; scale effects; full-scale ship hydrodynamics; CFD.*

1. Introduction

To guarantee the performance of a ship in the real world, naval architects routinely perform calculations to predict the behaviour of a prototype. Engineering design is usually an iterative process beginning with low fidelity analysis tools which increase in complexity as the design is finalised. A key prerequisite of a successful prototype is the availability of sufficiently mature tools to approximate the real environment as closely as possible. Regardless of the confidence the naval architect may have in an analysis tool, experiments are typically performed at a reduced scale. These model-scale experiments aim to represent real-world prototypes and can be used to hone in on a final design while bypassing possible modelling assumptions and simplifications such as the neglect of non-linear phenomena or viscous effects in calculations.

Economic pressures, or the availability of facilities, space, and time frequently result in intentionally small models, which may attract non-negligible differences with respect to the full-scale prototype. These differences can be split into three categories (Heller, 2011):

1. **Model effects:** a result of incorrect reproduction of geometrical features, flow properties such as turbulence, or wave characteristics.
2. **Measurement effects:** a consequence of dissimilar techniques of data collection between model and prototype. For example, De Rouck et al. (2005) report on the influence of measurement location and related uncertainties on wave overtopping predictions.
3. **Scale effects:** a result of disparities in force ratios acting on model and full-scale structures.

A key challenge for engineering design based on experimentation or numerical modelling is to determine the relative contributions of model, measurement, and scale effects. Large scale factors cause large scale effects, meaning that a model may not represent a prototype well. Yet, this has not discouraged the construction of so-called micro-scale experiments to study, for example, moveable beds reduced dimensionally up to 20,000 times (Maynard, 2006). In ship hydrodynamics there is no need to resort to such large scale factors. Nevertheless, scale effects are a source of considerable uncertainty, negatively impacting the development of technology and innovations that may improve operational performance, such as energy saving devices.

Todd (1965) described the problem concisely: *“It is believed that if we knew more about the true method of prediction from model to ship, and had greater confidence in the resulting estimates of ship power, these allowances [correlation allowance] could be reduced and a lower powered engine employed.”* This problem persists today. It is possible to obtain thousands of unique predictions for the full-scale power requirements of a vessel depending the method employed to calculate each constituent component of the total resistance (Terziev et al., 2019).

The principal difficulty arises due to the inherently complex nature of fluid flow. Even though naval architects are equipped with highly advanced modelling approaches and commercially available software, understanding and predicting fluid flow remains difficult. The main tool in a naval architect’s arsenal in this respect is Computational Fluid Dynamics (CFD) software solving the Navier-Stokes equations to predict the flow around a ship. There are now a number of commercially available such solvers, and coupled with the ever-increasing availability of computational power, uncertainties due to scale effects ought to reduce. Following this line of reasoning suggests that routine, high-quality analysis directly at full-scale without the need for experimentation will become the norm. Within this review, we aim to explain

the reasons why this is not yet the norm, and may not become the norm for some time by examining the phenomenology of scale effects acting on the resistance of a ship, and the computational and conceptual developments necessary to bypass them.

The remainder of this article proceeds by giving background to the physical origin of scale effects and summarising existing research in ship scale effects. Then, focus shifts to the obvious solution: full-scale numerical simulation. Here, particular emphasis is placed on the problems and challenges, which are split into turbulence modelling, computational power requirements, and the lack of data for validation. Finally, conclusions and recommendations for future research are summarised.

2. Scale effects and resistance extrapolation in ship hydrodynamics

Scale effects arise due to dissimilarities in force ratios between model and full-scale ships. Assuming one is able to reproduce geometrical and dynamical features correctly, similarity between only two dimensionless groups is necessary: the Froude number and the Reynolds number, shown in Eq. (1) and Eq. (2), respectively:

$$F_n = V/\sqrt{gL} \quad (1)$$

$$Re = VL/\nu \quad (2)$$

where V is the ship speed, g is the acceleration due to gravity, L is the ship length, and ν is the viscosity. The Froude number represents the ratio of inertial and gravitational forces and is associated with wave making. On the other hand, the Reynolds number indicates the ratio of inertial and viscous forces. Moreover, it serves as an indicator to whether flow is laminar, transitional or turbulent. If a hull is scaled for the purpose of an experiment, the dissimilarity between either F_n or Re is unavoidable for a model and prototype, leading to scale effects.

2.1 Extrapolation procedures

Ship resistance at model scale can be used to predict the full-scale power requirements. This is known as resistance extrapolation. A number of approaches to solving this problem are available today, but this review will confine its attention to the most widely used methods. Alternatives include Telfer's (1927) method which is based on geosim (geometrically similar) series, and Ferguson's (1977) approach of using signage and trim coefficients to describe the resistance curve and predict its scale effects.

2.1.1 Froude's method (2D approach)

Scaling of ship models may be done following Froude's approach, which assumes that the total resistance R_T of a ship may be decomposed as follows:

$$R_T = R_F + R_R \quad (3)$$

where R_F is the skin friction resistance and R_R is the residuary component, made up of wave, R_W , and pressure form resistance, R_P . In dimensionless form, the resistance components may be written as $C_T = C_F + C_R$ (achieved by $C_{T,R,F} = R_{T,R,F}/(0.5\rho S_w V^2)$, where S_w is the wetted area and ρ is the water density). Froude assumed that any change in the resistance coefficients of the model and ship operating at the same Froude number arise due to changes in the frictional resistance coefficient (C_F), which is solely dependent on the Reynolds number. This frictional component may be estimated by using a friction line, for example, the ITTC'57 correlation line. The chief difficulty lies in establishing an approach to estimate R_R prior to the experiment, and splitting it into its constituent components. Since R_R contains both viscous and wave effects, it is notoriously difficult to predict. In fact, a theory able to predict R_R was formulated for the first time only recently (Gotman, 2020).

2.1.2 Hughes' method (the form factor method, or the 3D approach)

An alternative to Froude's method of subdividing the total into two components is the form factor ($1 + k$) approach, suggested by Hughes (1954) and recommended by the 14th International Towing Tank Conference (ITTC). This essentially consists of splitting the residual resistance into a form resistance and a wave resistance (C_W):

$$C_T = (1 + k)C_F + C_W \quad (4)$$

It is assumed that $(1 + k)$ is independent of speed and scale, i.e. Re, F_n . However, there is abundant experimental and computational evidence to show that the form factor does indeed depend on the Reynolds number (García-Gómez, 2000; Terziev et al., 2019). For example, the results of Min and Kang (2010) demonstrate the maxim 'the higher the scale factor the larger the scale effects' well. Their work showed experimentally that at low Reynold numbers (high scale factor), $(1+k)$ changes at a higher rate than at large Reynolds numbers.

2.2 The missing link

Dimensional analysis to the first order suggests that all terms have been accounted for in the approaches examined above. However, an interaction term between the Froude and Reynolds number is also known to exist, formulated by Molland et al. (2017) as follows:

$$C_T = f_1(Re) + f_2(F_n) + f_3(ReF_n) \quad (5)$$

with $f_{1,2,3}$ being some functions presumably dependent on the hull shape and size. In essence, Eq. (5) postulates that resistance is made up of a term depending on the

Reynolds number, a term depending on the Froude number, and a term depending on both, i.e. an interaction term.

2.2.1 Evidence to support the existence of an interaction term

There are good reasons for believing Eq. (5) represents the physics of ship resistance better than suggested by either of the previously examined methods. All known components of ship resistance can change as a result of variation in Froude and Reynolds number. For example, altering the Reynolds number causes the boundary layer of a hull to change thickness (White, 2006). This thickness does not change linearly with the scale factor. Therefore, the displacement thickness, pressure, and velocity distribution within the boundary layer is dissimilar at varying scales. Clearly, these physical differences will impact wave resistance, rendering C_W a function of the Reynolds number as well as the Froude number.

Additionally, the total resistance of a hull may contain more components than those examined previously. For example, interaction terms in multihull vessels, or Baba's (1966) viscous component caused by the expended energy to create turbulence due to bow wave breaking. Such a component of resistance depends on the Froude number, since at low F_n , there is no wave breaking and therefore no corresponding resistance component. It also depends on the Reynolds number through turbulence, which is described through the Re rather than the F_n .

2.2.1.1 The wave resistance coefficient and its Reynolds number dependence

In the past, the varying displacement thickness of a boundary layer at different Reynolds number has been exploited by researchers seeking to improve wave resistance estimates. Since the displacement thickness can be approximated by known equations describing 2D flat plate boundary layers, it is possible to modify the shape of the hull to include the displacement thickness distribution (Lazauskas, 2009).

Accounting for the displacement thickness of a ship's boundary layer in an otherwise inviscid fluid certainly improves predictions, but cannot fully account for the difference with experiments fully (Brard, 1970). Moreover, this approach does not take into account the true interaction between viscosity, vorticity and turbulence on ship waves. As explained by Dand (1967), one way to illustrate this is to consider the wave resistance of a vessel going ahead and going astern. Potential flow theory would suggest the wave resistance is identical in both cases, but this is not what happens in reality. The disturbance generated at the bow causes chaotic turbulent flow to be shed towards the stern where it modifies the instantaneous and mean wavemaking ability. The differences in flow properties between a vessel moving ahead and astern will therefore snowball as they cascade downstream in each case, explaining why the downstream perpendicular is always weaker in producing waves. Even if the varying

thickness of the boundary layer were to be accounted for, the turbulent length scales are different at low and high Reynolds numbers (Durbin and Pettersson Reif, 2011). This results in a broadening of the turbulent kinetic energy spectrum, meaning that eddies of different sizes are interacting with the wake and wave system at different scales.

In the 1970s, the first theories targeted at solving a wake with viscosity or vorticity appeared. Tatinclaux (1970) appears to be the first to devise a mathematical theory which incorporates vorticity effects on ship waves. Concurrent with Tatinclaux's (1970) work, Brard (1970) predicted that effects of viscosity on a ship's near-field waves vary as $(Re \times F_n^2)^{-1/3}$, while far-field waves vary as $(Re \times F_n^4)^{-1}$. Both physical insight and these formulations agree that near-field disturbances are influenced by scale effects to a greater extent. This agrees with observations of ship wakes which show that the Kelvin wake is influenced insignificantly by changes in the Reynolds number. A short time later, Beck (1971) produced a thin ship linear mathematical framework where a viscous wake is accounted for as a region of vorticity trailing behind the ship. He derived analytical relations for the wave resistance and showed a viscous contribution of up to 10%.

It is therefore surprising that soon after the aforementioned studies were published, the opinion that wavemaking resistance is independent of viscosity began forming. This opinion partly persists today, particularly in standard references for educational purposes many of which were composed at the time. Ironically, it was computational power that led to such conclusions. Soon after the introduction of Michell's (1898) integral for wave resistance in naval architecture circles, it became apparent that experimental wave resistance results oscillate less than would be suggested by Michell's (1898) integral.

Michell's (1898) approach formulates the fluid as linear, inviscid and irrotational, and the body (hull) as thin. It also requires the linearisation of the free surface and body boundary conditions. As soon as exact boundary conditions (Baar and Price, 1988) were implemented in computer codes, predictions became much better at approximating experimentally determined residual resistance. According to Landweber and Patel (1979), these improvements were falsely seen as a vindication of Froude's law, primarily because residuary resistance is not wave resistance. The improvement was a direct result of the relaxation of some of the assumptions, but crucially, not all assumptions were removed.

There are many other good reasons for insisting that viscous effects contribute to wavemaking, which naturally lead to scale effects. For example, the first viscous modification to Michell's (1898) integral was by Havelock (see Wigley (1965)). He found that incorporating such effects reduced the oscillation of the wave resistance

curve with varying F_n , resulting in better agreement with experimental data – in a very similar way to what was achieved by including the exact boundary conditions. Similar conclusions can be found in Gotman (2002). Beck (1971) also reached Havelock's conclusion: viscosity reduces oscillations in the wave resistance curve and brings results closer to experimental data.

There are flow and pressure distribution factors to be considered in conjunction with the above arguments. For example, the presence of vorticity, associated with the free surface boundary layer and surface curvature, is thought to play an important role in determining the height of the wave at the stern (Landweber and Patel, 1979). Although vorticity affects the bow wave through wave breaking, it is not included in 'exact' boundary conditions. The presence of the free surface also modifies the pressure distribution on the hull considerably when compared to a double model (also known as a zero-Froude number case where the free surface does not exist and the body is treated as deeply submerged). Moreover, the viscous pressure resistance coefficient varies with Froude and Reynolds number (Terziev et al., 2021a).

Many of the problems examined within this section are problems of the past and it is increasingly rare to see research on this topic. Partly, because highly accurate results can be obtained with reasonably little effort through Navier-Stokes methods, and partly because of the mathematical difficulty in expressing all properties of the flow around a hull.

2.2.1.2 The form factor and its dependence on F_n and Re

As mentioned earlier, the form factor's Re dependence is well known from experimental and computational research. Since the form factor represents form resistance, it is natural that a varying boundary layer thickness with changing Re will influence its magnitude. However there is considerably less research on F_n dependence of the form factor. There are two possible lines of reasoning one can take in exploring Froude number dependence of the form factor. Both approaches rely on sinkage and trim, but they do so from different viewpoints and reach opposite conclusions.

Sinkage and trim are known to change relatively little with the Reynolds number. For example, Kok et al. (2020) used CFD to investigate self-propelled squat and its scale effect. While they concluded that a negligible scale effect exists, an analysis of their results shows approximately 5% difference in dimensionless squat at model and full-scale, which is certainly non-negligible. Typically, such changes are obscured by other uncertainties, or their effects on resistance absorbed within the correlation allowance. This means that scale effects on sinkage and trim remain somewhat controversial.

While very little research exists on the topic, changing the wetted surface area or trimming a vessel unevenly will clearly impact the form resistance (Ridgely-Nevitt, 1959). Since sinkage and trim change considerably with Froude number, it is conceivable that form factor variations as a result of varying Froude number are a secondary effect we can correct for by modifying the mean flow velocity around the hull. This was Yokoo's (1960) approach to the problem, who presented correction formulas to modify the mean flow in an attempt to account for these phenomena. To the best of the authors' knowledge, these corrections remain untested in the literature. Under this framework, there are no 'true' Froude number effects on the form factor. Instead, there are changes to $(1 + k)$ for each trim and draught condition.

Ferguson (1977) disagreed with the above assessment. He argued that Froude number influences on the form factor are not a secondary effect. Instead, he cited Dand's (1967) discovery of scale effects (varying Re at a constant F_n) on the vertical force and trimming moment causing sinkage and trim, respectively, as evidence. Ferguson (1977) agreed that the form factor differs due to sinkage and trim, but he argued that such effects are caused by scale effects resulting from 3D (form effects) on sinkage and trim. So, the cause of scale effect in sinkage and trim is the form resistance itself. In essence, Ferguson (1977) saw a single phenomenon based largely on boundary layer physics and experimentation where Yokoo (1960) saw two. Although he did not explicitly state so Ferguson's (1977) conclusions are in direct contravention to established extrapolation laws. On the other hand, Yokoo (1960) found a way to preserve the validity of these hypotheses by devising correction factors.

To further investigate the presence of an interaction term, it is instructive to observe effects of the Froude number on the form factor from a CFD perspective. This is what Terziev et al. (2021) set out to investigate using the so-called double body simulation technique. In double body simulations, the free surface is replaced by a symmetry plane, eliminating C_w from Eq. (4) and allowing the direct computation of the form factor. Terziev et al. (2021) studied the KRISO containership (KCS) in 4 different scale factors, at 14 speeds ranging from $F_n = 0.02$ to 0.28 (with $F_n = 0.26$ being the design speed of the KCS), and modelled three widely used turbulence models. They found that at low speeds, the form factor is subject to considerable variation which is highly sensitive to the turbulence model at all scales. On the other hand, once the ship speed is higher than approximately $F_n = 0.15$, the difference in the form factor with increasing F_n becomes negligible. While the discretisation uncertainty was highest for the low speed cases, Terziev et al. (2021) also demonstrated that full-scale results described the smoothest curves regardless of the turbulence model employed. However, their assessment did not include varying trim and sinkage; this is therefore recommended as a future piece of research.

Nevertheless, they narrowed down the search for F_n dependence on the form factor considerably – it is now known that past a certain speed range ($1 + k$) is essentially F_n independent. The viscous pressure resistance was also shown to depend on F_n and Re . It is now necessary to remove the discretisation uncertainty element to determine whether scale effects take place at low F_n .

The abovementioned results likely point to the need for transition modelling at low speeds. The approach to how this is done is also recommended as a piece of future work. Turbulent-laminar transition is controlled by the Reynolds number, but its simulation is not straightforward, causing some uncertainty.

Uncertainty, albeit of a different type and cause, plagues experimental form factor determination just as it does in CFD. This makes it possible that some of the differences attributed to scale effects may be alleviated by underlying uncertainties or absorbed in correlation allowances. An account of the pertinent background and issues are explored by Korkmaz et al. (2021). Since the Prohaska test is carried out at low speeds, the combination of experimental and numerical uncertainty obscure the presence or absence of scale effects. Typically, a high scale factor (λ , meaning low Re) corresponds to a high uncertainty (Zhao et al., 2020).

2.3 Shallow and confined waters

Mathematicians frequently apply their models to limiting cases seeking to understand behaviours in general. Following this line of reasoning, it is informative to examine scale effects in shallow and confined waters. In such cases viscosity plays a much greater role than in unrestricted waters (Tuck, 1978). Since viscosity is the reason why we observe scale effects in the first place, studying confined waters can reveal information about the nature of scale effects by magnifying their relative importance and making them easier to detect.

For example, the study on squat by Kok et al. (2020) was carried out for very shallow water cases (depth to draught ratios as low as 1.1). Such studies are valuable because they reveal small but nevertheless important aspects of the physics of scale effects one might not have been able to detect in deep waters where the magnitude of sinkage and trim is typically much smaller. However, it is also instructive to examine whether experimental evidence exists to support scale effects in sinkage and trim.

One of the most widely used hulls for experimentation and validation purposes is the KCS hull. While few experiments study its performance in shallow water, there is experimental evidence of significant disagreement between testing facilities at different scales. For example, Shivachev et al. (2017) measured a trim of 0.162° at a scale factor of $\lambda=75$, while Simonsen et al. (2013) reported a trim of 0.185° for $\lambda=52.667$ at the same Froude number: a difference of more than 12%. While there are many other

possible explanations for this difference, we certainly cannot exclude the presence of scale effects. To the best of the authors' knowledge, this is a unique example of openly available experimental data of a hull tested at different Reynolds numbers. Since the experimental facilities where the tests were conducted likely have different procedures and approaches, the uncertainty between the two should be evaluated (Youden, 1972).

Another reason why shallow and confined waters are known to exhibit a greater scale effect is the interaction with the seabed. As explained earlier, the near field disturbance is influenced by scale effects to a greater extent. This, combined with the fact that a boundary layer may form on the seabed itself explains why one should expect a magnified scale effect (Shevchuk et al., 2016). Consequently, at different scales, flow properties in the gap between the hull and seabed or canal sides vary according to the Reynolds number and not the linear scale. This means that testing at different factors creates the possible interaction between two boundary layers – one formed at the seabed as a result of the locally accelerated flow and one shed from the hull. Since the flow is retarded more at low Reynolds numbers due to the relatively thicker boundary layers, the effective blockage is also influenced.

Shallow water studies have also shown counter-intuitive behaviour of the form factor and wave resistance coefficients. Since viscous effects are of lesser importance at higher Reynolds numbers as a result of relative thinning of the boundary layer, one might expect the increase in form factor and C_W observed in deep waters to be replicated in shallow waters. However, this is not the case. Zeng et al. (2019) showed that form factors decrease in shallow water with increasing Reynolds number. They suggested that while viscous effects decrease in such a scenario, vortex effects increase. Terziev et al. (2021b) demonstrated that these parameters reduce following a path similar to those described by the near and far field relations devised by Brard (1970). Namely, a significant difference in $(1+k)$ and C_W can be observed between $10^6 < Re < 10^7$, with little scale effect thereafter. This Re region also corresponds to where experiments are carried out, and according to Zhao et al. (2020), low Re are associated with higher uncertainty. While it is true that vortex formation is delayed in full-scale, it is not immediately apparent how this influence grows in anything other than relative importance as the Reynolds number is increased.

2.4 Can existing ship resistance components account for $F_n - Re$ interactions?

Thus far, scale effects were examined on the wave resistance and the form factor. Since these two terms have received considerable attention by researchers, it was important to devote sufficient time examining them. Before delving into the matter of whether existing components of ship resistance can account for $F_n - Re$ interactions, it is

important to examine one final aspect at the heart of the resistance extrapolation problem. Specifically, the estimation of frictional resistance.

The form factor is defined as the ratio of the viscous resistance coefficient and the flat plate resistance coefficient at the same Reynolds number. There are two conceptual problems with this definition:

1. The ITTC'78 procedure is calibrated to use a correlation allowance in conjunction with the ITTC'57 correlation line. Since the correlation line is not a flat plate line and contains a 'form factor' itself, this definition is not actually satisfied.
2. There is still no agreement as to which friction line actually represents the resistance of a flat plate, causing some variation in the approach taken to compute C_F . Such approaches continue to be developed using numerical methods (Eca and Hoekstra, 2008; Korkmaz et al., 2019; Wang et al., 2015). By our count, there are at least 20 different friction lines expressing C_F as a function of Re^1 . Although predictions from these lines may coincide for specific Reynolds numbers (i.e. the curves they describe intersect), they typically provide unique values. This is illustrated in Figure 1, which also contains the standard deviation of the friction lines at each Reynolds number. As is evident from this figure, the largest disagreement is found in the low Reynolds number range, where the form factor is estimated experimentally. A comparison of the effect the choice of friction line can be found in Park (2015).

These problems were recognised early on: the adoption of the ITTC correlation line included what is essentially a disclaimer that this was a temporary solution – one that was designed to fill an immediate gap with the intention that this will be improved upon. Yet, theoretical advances in this direction have all but stalled. In part this is because of the probably unexpected at the time success of the ITTC line. Even today, it is frequently used to compare CFD predictions of frictional resistance coefficients and has even been used as a measure of accuracy.

The form factor's problems were seen early on by experimental facilities. Today, most of these facilities, particularly the more commercially-oriented ones (as opposed to small educational or research facilities), rely on large datasets of experiments they have performed and corresponding sea trial results. They prefer using these datasets

¹ For example (arranged alphabetically): Date and Turnock (1999); Gadd (1967); Grigson, (1999); Hughes (1954); Katsui et al. (2005); Korkmaz et al. (2019); Lap (1956); Lazauskas (2009); Prandtl (1925); Schoenherr (1932); Schultz-Grunow (1941); Telfer (1927); Wang et al. (2015); White (2010). Note that some of these references contain more than one proposal for a friction line. Schlichting (1979) also lists a number of alternatives included in Figure 1.

as opposed to the ITTC recommended method because of the problems associated with extrapolation procedures.

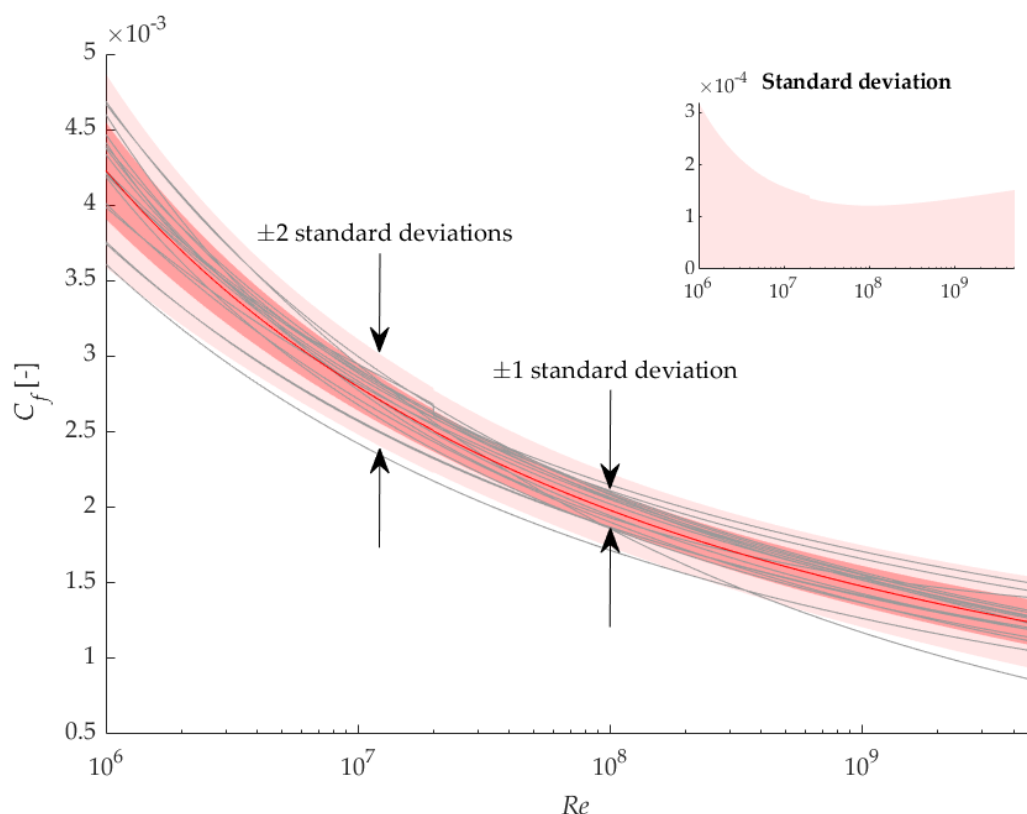


Figure 1. Frictional resistance coefficients predicted using a variety of friction lines. This figure contains the mean of all frictional resistance coefficient predictions (red line), along with ± 1 and ± 2 standard deviations. The standard deviation of all methods is greatest for low Re . Friction lines are represented by grey lines¹.

The reason why many industry bodies opt to disregard official recommendation can be summarised as follows:

- The extrapolation procedure is not valid for immersed transoms.
- The extrapolation procedure ceases to be valid for separated flows, which may occur suddenly as the F_n is increased. Moreover, this may occur at different Froude numbers at model and full-scale since the flow is modified by turbulence, viscosity, and vorticity causing potential disparities in the height of the free surface at the stern.
- The components supposed independent of viscosity can affect viscous components, for example, waves modify the dynamic pressure and flow influencing boundary layer physics and viscous pressure resistance (ITTC, 1999). Also, waves may influence the presence or location of separation (Chow, 1967; Zhang and Stern, 1996), so in certain cases, the extrapolation procedure may be invalid for some, but not all Reynolds numbers.

- The extrapolation procedure must be modified for novel hull forms.
- The extrapolation procedure is not valid for shallow and confined waters.

To exemplify the problems of the extrapolation procedure further, it is instructive to consider free surface effects on frictional resistance coefficients. The presence of a free surface modifies vortex shedding patterns, turbulence and vorticity along with the dynamic pressure and separation changes mentioned earlier. Existing scaling laws cannot account for these complex physics.

These items point to the fact that existing components of ship resistance are likely incapable of accounting for all scale effects. The main reason for such a conclusion rests in the fact that the resistance breakdown is linear. While the success of these procedures suggests that linear effects dominate ship resistance scaling, non-linear components and interaction terms certainly exist. Linear terms are unable to produce behaviours in the physical system a non-linear breakdown could, so this is an expected consequence.

3. Computational Fluid Dynamics

The past few decades have seen explosive growth in the use of CFD methods based on Navier-Stokes equations. This has allowed the honing of techniques and procedures to predict ship resistance at model scale with excellent accuracy (Hino et al., 2020; Larsson et al., 2014, 2003). In large part, these efforts were helped by the existence of benchmark geometries and high-quality validation data. A prime example is the KCS hull, which has been subject to numerous experiments (Elsherbiny et al., 2019; Lee et al., 2003; Shivachev et al., 2017; Simonsen et al., 2013). This has allowed the research community to determine the best practice approaches for modelling ship hydrodynamics at model scale.

3.1 Computational bottlenecks

This section seeks to explore some of the issues, both practical and conceptual, where current research efforts are likely to yield improved modelling practices. These include turbulence modelling, computational power, and discretisation uncertainty. Although distinct, these issues are interconnected and deal with many of the issues.

3.1.1 Early problems

Before the turn of the century, CFD modelling was primarily two dimensional and in the steady state. Steady state simulations are highly useful and practical, particularly because they provide the fully nonlinear solution of the governing equations while requiring relatively little computational effort. The main problems with modelling ship flow in the steady state can be split into two:

1. **Free surface hydrodynamics:** The most widely adopted free surface modelling technique, the Volume of Fluid method (Hirt and Nichols, 1981), requires an unsteady set up. This issue, and other techniques to model an air-water interface are discussed at length by Wackers et al. (2011). The inability to model free surfaces inherently restricts analysis to steady motion and cannot account for dynamic trim, sinkage, nor seakeeping and manoeuvring.
2. **Large-scale motions within the flow:** Assuming an eddy-viscosity turbulence model is used, applying an unsteady solution procedure to a superficially statistically steady case may reveal large-scale motion within the flow. When averaged over long periods of time, these motions may exhibit behaviours which are distinct from those obtained via steady state simulations (Runchal, 2020). Typically, such procedures also lead to better agreement with experimental data. While unsteady RANS (URANS) is considerably costlier than RANS, the requirements are at least one order of magnitude lesser than Large Eddy Simulation (LES) approaches.

Steady state free surface hydrodynamic flows have been achieved in some special cases, but these are not widely available making them of lesser relevance. On the other hand, double body simulations are popular even today in the study of ship flows. Wave resistance can have a low relative contribution to the total, so eliminating C_W is sometimes justifiable. Moreover, many accessible methods are available that can estimate C_W separately. Double body simulations also allow the prediction of the form factor. Such simulations were the first to be used, particularly at Reynolds numbers corresponding to full-scale ship flows.

3.1.2 Grid numbers and turbulence

While multiphase simulations are commonplace today, the problem of computational power availability is not yet resolved. The drive to resolve ever smaller turbulent length scales is one of the main reasons why ship CFD practitioners seek increasingly large grid numbers. For example, Liefvendahl and Fureby (2017) give a number of formulations expressing the near wall grid numbers and estimated wall modelled LES at typical full-scale Reynolds numbers requires between 2.5×10^9 and 9.7×10^9 cells, while wall resolved LES necessitates between 4.9×10^{12} and 67×10^{12} cells. Such grids are too difficult to produce and handle even in research contexts, let alone practical applications.

The need to resolve parts of the turbulent kinetic energy spectrum is not limited to RANS/URANS and LES. Bridging techniques have emerged, such as Detached Eddy Simulation (DES), where the boundary layer is modelled using an eddy-viscosity turbulence model, while the larger scales of motion in the free stream are resolved using a LES approach. This method has considerable advantages to URANS and has

been shown to provide good results in a variety of applications (Nisham et al., 2021; Pena et al., 2019).

The principal issue with applying DES is that the method is not inherently adaptive. That is, DES simulations will not converge to Direct Numerical Simulation (DNS) results, where the entire turbulent kinetic energy spectrum is resolved if a sufficiently fine grid and time step are used. In essence, the DES approach relies on the existence of a URANS boundary layer. On the other hand, recently emerging methods, such as Partially Averaged Navier-Stokes simulations (PANS) (Girimaji and Abdol-Hamid, 2005; Vaz et al., 2017; Zhang et al., 2018) and Scale Resolved Hybrid (SRH) turbulence modelling (Duffal et al., 2019; Fadai-Ghotbi et al., 2010; Manceau, 2019) do not suffer such problems. The SRH approach in particular uses an eddy-viscosity turbulence model and adaptively switches to LES where and when the grid size and time step allow accurate resolution of turbulent length scales, thereby converging to DNS for sufficiently fine grids and time steps. SRH and PANS approaches are potential game changes in ship CFD because of their inherent adaptability which removes part of the decisions the analyst must make in setting up the simulation.

3.1.2.1 The near-wall grid

It is frequently the case that URANS solutions are sufficient to provide accurate integral properties, such as ship resistance. This is particularly the case at full-scale where the Reynolds number may be in the region 10^9 , and solving on a sufficiently fine grid to resolve turbulent structures may not be an option due to limited resources. In such cases, one of the main dilemmas with regards to modelling one must decide on is the near-wall grid strategy. There are two approaches in this respect: resolving the viscous sublayer (corresponding to $y^+ < 5$) and using wall functions (corresponding to $y^+ > 30$). It is usually desirable to resolve the viscous sublayer, since the use of wall functions carries additional assumptions.

Grid resolution below $y^+ = 5$ is usually recommended for scale resolved simulations (Spalart, 2001). However, examples of full-scale ship hydrodynamics with corresponding y^+ values are rare. This is because of the scaling of grid requirements with Reynolds number. If the same number of near-wall layers were used for a model and full-scale simulation, the resulting y^+ would vary by a factor $\lambda^{1.35}$, with λ being the scale factor (Peric, 2019). Assuming a λ of 50 and y^+ of 1 at model scale gives $y^+ \approx 200$ if one simply scales the grid with λ . Reducing the wall-normal direction only is not always advisable, since high cell aspect ratios may cause divergence.

To set grid properties, one can use information from the ITTC correlation line (C_f , given in Eq. (6), or indeed, any other approach expressing the friction coefficient as a function of Re). This is used to estimate the shear wall stress, τ_w (given in Eq. (7)) and give the first layer thickness ($2\Delta y$, given Eq. (8)). The number of the near-wall layers

(n , given in Eq. (9)) can be estimated assuming a flat plate boundary layer thickness, δ , given in Eq. (10).

$$C_f = 0.075/(\log_{10} Re - 2)^2 \quad (6)$$

$$\tau_w = C_f \rho V^2 / 2 \quad (7)$$

$$\Delta y = y^+ v / u_t \quad (8)$$

$$n = \log \left(1 - \frac{\delta(1-S)}{2\Delta y} \right) / \log(S) \quad (9)$$

where $u_t = \sqrt{\tau_w / \rho}$ is the friction velocity, and S is the common ratio in the geometric series whose sum equals δ (approximated using Eq. (10)), used to describe the distribution of layers. The coefficient of this geometric series is half of the first layer thickness, $2\Delta y$. The factor 2 appears here because we wish the cell centre to be at a distance of Δy rather than its vertex.

$$\delta = 0.382L / Re^{1/5} \quad (10)$$

To demonstrate the effect of Reynolds number on the near-grid properties, Eq. (6) – Eq. (10) are used on the KCS for its operational speed, corresponding to $F_n = 0.26$ and scale factors between 1 and 100. The target y^+ value is set to 1, 2, 3, 5, and 30, while the common ratio, S , is varied between 1.1 and 1.4. The resulting geometric series has a total thickness equal to δ ($\delta \approx 1.1 \text{ m} \approx 0.48\%L$) regardless of y^+ or S values, although near-wall layers may extend for a smaller distance in practice (for example, 0.5δ , or even 0.1δ). This is used to illustrate the effect of the Reynolds number on the near-wall grid requirements and highlights the difficulty in achieving even $y^+ = 30$ in full-scale. The resulting Δy values are depicted in Figure 2, while the number of layers for each common ratio are depicted in Figure 3.

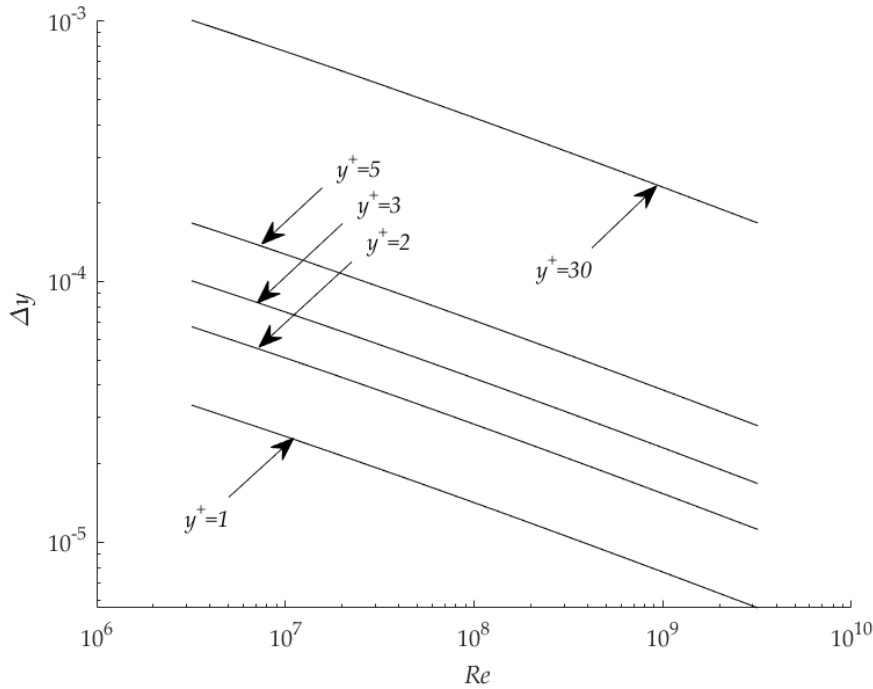


Figure 2. First layer thickness requirements to maintain constant y^+ values of 1, 2, 3, 5, and 30 for Re corresponding to the design speed and scale factors between 1 and 100 for the KCS. These values are computed using Eq. (8).

One may query whether it is necessary to maintain grids with the exemplified y^+ values at full-scale. This depends on the solver's ability to re-create velocity and turbulent properties for a given y^+ value. Typically, wall functions are fitted to experimental or DNS data. The problem with this has been that it is exceedingly difficult to conduct either experiments or DNS to provide data for very high y^+ . However, such data exists for y^+ up to 10^5 , which shows the log layer law maintains its validity well (Lee and Moser, 2015). At full-scale, it is therefore possible to place the first cell comparatively further than in model-scale, say at $y^+ = 1000$ or even higher, in which case, the entire near-wall layer (of thickness δ) will be discretised with between 12 and 30 cells depending on the value of the common ratio, S . Each of these cells will allow a much larger surface element size, measuring up to about 1m and allowing a considerable reduction (several orders of magnitude) in overall cell numbers. That is, provided the geometry can cope with large elements and any curvature is represented accurately.

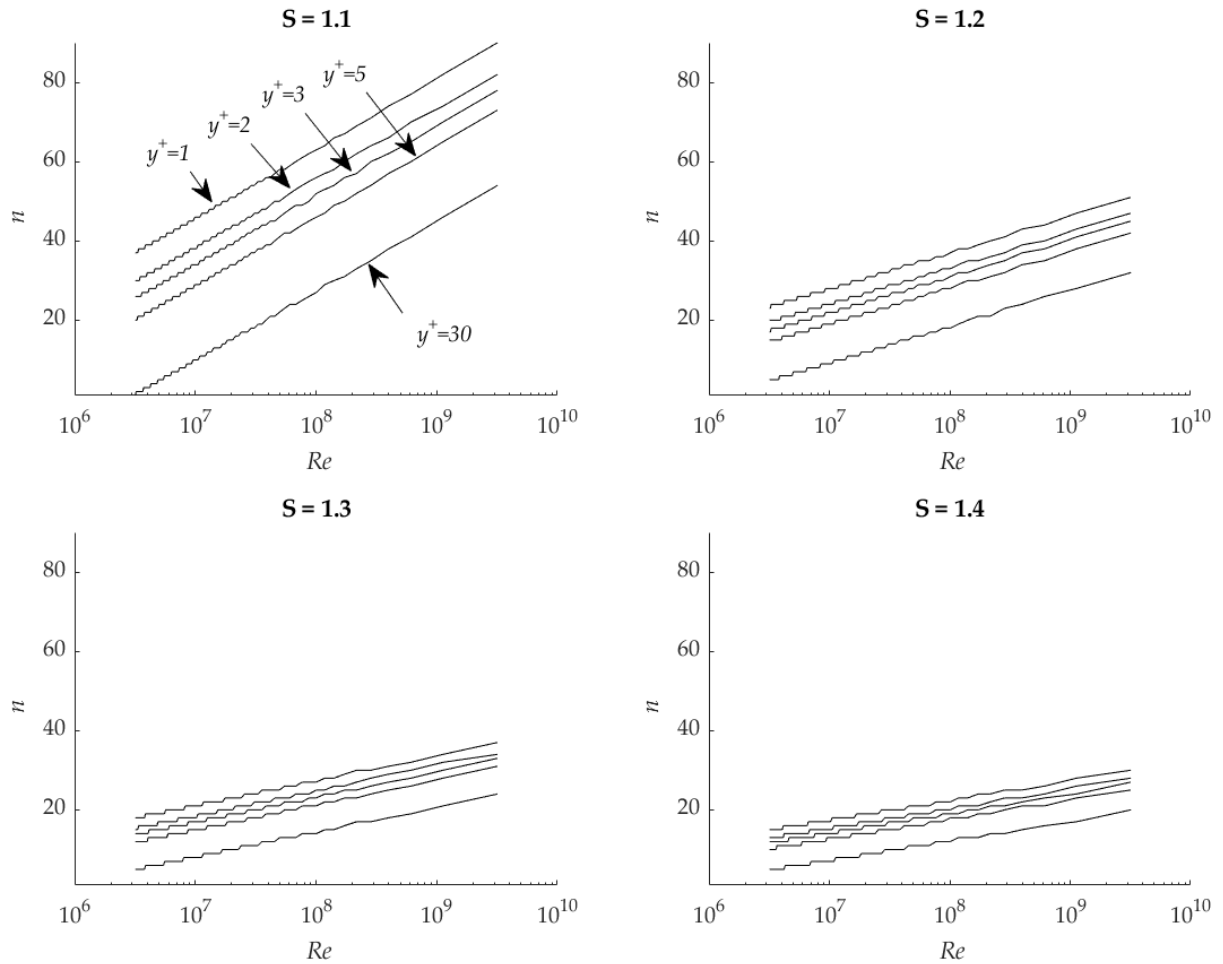


Figure 3. Number of layers required to maintain a constant y^+ value based on common ratios, S , of 1.1, 1.2, 1.3, and 1.4. The value of n is rounded up to give integer values for each Re corresponding to the design speed and scale factors between 1 and 100 for the KCS. These values are computed using Eq. (9). Each line represents a constant y^+ , which descends in magnitude with increasing n in all cases, as shown in the tile corresponding to $S = 1.1$.

To the best of the authors' knowledge, one of the most comprehensive studies assessing the influence of wall functions on flow properties was carried out by Eca and Hoekstra (2011). They assessed the influence of y^+ on the frictional and pressure resistance coefficients, as well as the wake of a hull at model and full-scale Reynolds numbers. The findings of Eca and Hoekstra (2011) showed that discretisation uncertainties spike in the buffer region $5 < y^+ < 30$, and particularly around $y^+ = 15$. The pressure resistance coefficient showed significant deviations for these y^+ values as did the wake at model-scale. However, their results show that at full-scale the y^+ dependence is much weaker while retaining a relatively strong dependence on the turbulence model used. These findings justify the use of wall functions and high y^+ at full-scale.

3.1.2.1.1 Surface roughness and fouling

A key consideration in choosing the near wall grid is modelling roughness. Ship resistance can vary considerably when surface roughness is introduced and compared to hydraulically smooth hulls (Demirel et al., 2017).

Modelling surface roughness is a highly complex field in its own right. This review will therefore not delve into the intricacies of the subject, rather, a few key details are discussed and their influence on the near-wall grid. For an in-depth review of surface roughness and the hydrodynamic performance of fouled surfaces, the reader is referred to the in-depth analysis of Andersson et al. (2020).

There are three approaches to modelling roughness effects. These include low wall-distance-based Reynolds number approaches, high wall-distance-based Reynolds number approaches, and resolved methods. The low wall-distance-based Reynolds number approach relies on a low y^+ approach, i.e. wall functions are not employed. Instead, the turbulence model's boundary conditions are modified to account for the effect of roughness (Wilcox, 2006). The corresponding high Reynolds number approach is by far the most popular. In it, modelling roughness is achieved through of shift in velocity within the turbulent boundary layer by incorporating a roughness-dependent parameter (Demirel et al., 2014) in conjunction with wall functions. The final method resolves the geometrical characteristics of fouling directly (Wang et al., 2004).

Validation exercises can be found for all methods to model roughness, many of which are covered by Andersson et al. (2020). While the resolved method contains no additional assumptions with regards to the flow behaviour, the resolution of geometrical asperities for a ship (at the micro or nano scale) is beyond current capabilities. It is therefore important to comment on the roughness effect on turbulence and the wake.

For example, the effect of surface roughness on turbulent eddies, and whether these differ substantially when comparing modelled and resolved methods. The key problem here is that velocity shift-type approximation (as in the high wall-distance-based Reynolds number approach) of roughness modelling might be incapable of re-creating geometrical asperity-influenced eddies downstream if turbulent length scales are resolved outside the boundary layer (by a DES model for example). Alternatively, this re-creation might not be consistent with experiments, even though substantial experimental evidence supports the use of averaged methods for integral properties estimation such as resistance (RANS/URANS; for example, S. Song et al. (2019)). This line of reasoning is similar to that deployed in arguing against the use of wall functions in scale resolving simulations.

Varghese and Durbin (2020) shed light on this by rephrasing this problem in terms of Townsend's hypothesis. The essence of Townsend's hypothesis is that the large, energetic eddies existing some distance from the wall are independent of the surface condition. In other words, geometrical asperities only influence the Reynolds stress scale within a few roughness heights (McNaughton and Brunet, 2002). This idea rests on the premise that the roughness height is much smaller than the boundary layer thickness, which is certainly true for most cases. However, the presence of large barnacles may be problematic for this assumption. Varghese and Durbin (2020) demonstrated that similar turbulent properties are generated by a model with resolved roughness and one where roughness is included but not resolved (i.e. wall functions are used) when employing a Delayed Detached Eddy Simulation approach. They further proposed an extension to Townsend's hypothesis to explain the effectiveness of their approach by matching the roughness Reynolds numbers of either case (resolved roughness/modelled roughness).

The main conclusion from this section is that near-wall grid requirements differ substantially at model and full-scale. This can be exploited to further standardise the use of full-scale simulation. Moreover, some of the problems reported in the literature regarding wall function and roughness modelling may prove to be of considerably less consequence than currently thought.

3.2 Simultaneous Reynolds and Froude similarity without dimensional scaling

Haase et al. (2016b) proposed a method where full-scale Reynolds numbers are achieved by altering the value of viscosity of water, rather than the physical dimension of the vessel. They demonstrated that a good agreement with full-scale trials can be achieved in this way. Haase et al. (2016a) subsequently performed a similar assessment for a catamaran in finite waters. This approach, which satisfies F_n and Re similarity simultaneously, makes use of the previously stated fact that theoretically, ship resistance depends on only two-dimensional groups. One is free to manipulate any of the parameters F_n and Re depend on to achieve similarity, and not just the length scale L and velocity V .

The approach of Haase et al. (2016b, 2016a) allows unique insight into the physics of scale effects without the need for resorting to high cell numbers, making such investigations much easier to handle. However, the benefits of using this approach have been contested. Specifically, the original version of the method which we will call 'viscous scaling' preserved identical grids across the investigated Reynolds number range. The main benefit of using model scale simulations to begin with is that

a low y^+ average over the hull can be maintained, which is known to provide robust results.

When changing the Reynolds number, whether by dimensional scaling, or viscous scaling, one runs into the issues discussed earlier and illustrated in Figure 2 and Figure 3. Sezen and Cakici (2019) preserved the similarity in y^+ for model and full-scale Reynolds numbers, which eliminated the appeal of the method. However, other research has maintained identical cell numbers for model and full-scale Reynolds numbers and has showed boundary layer thickness (Figure 4) and resistance predictions are essentially identical using dimensional and viscous scaling (Terziev et al., 2021a, 2021b, 2019). These assessments include double body and multiphase simulations and show that the latter method requires fewer cells by about an order of magnitude while providing good agreement with dimensionally scaled simulations. As discussed earlier, allowing for high y^+ values, particularly at full-scale Reynolds numbers is justifiable, meaning that y^+ similarity is not a requisite for the method.

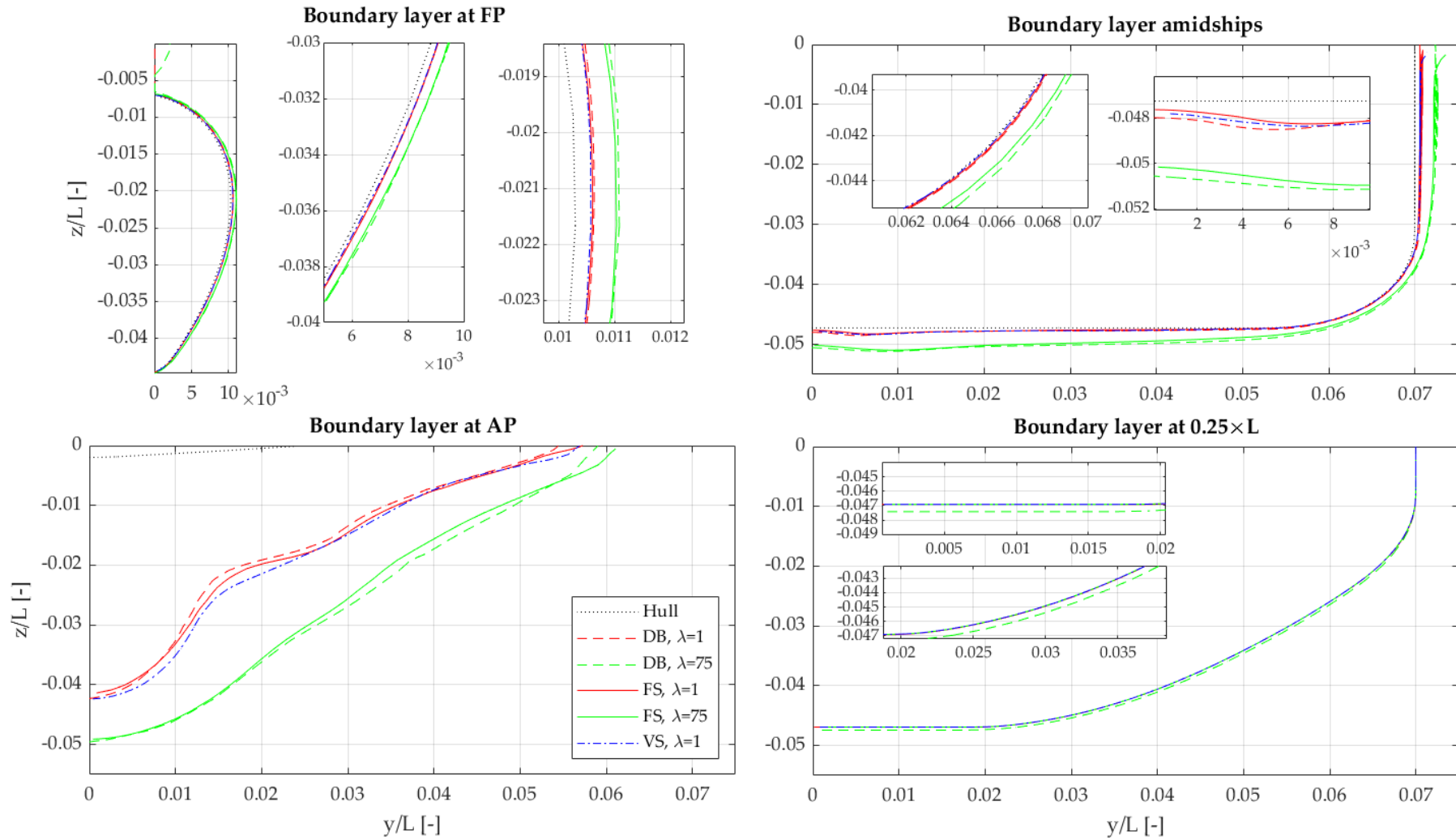


Figure 4. Boundary layer extents (90% of free stream velocity) predicted via a double body (labelled 'DB') approach, multiphase (labelled 'FS' representing 'free surface'), and viscous scaling (labelled 'VS', which was modelled in the multiphase regime at full-scale Re). The case study corresponds to the KCS hull, scaled by a factor of λ , as indicated in the figure legend in a confined water condition replicating the canal case of Elsherbiny et al. (2019) (canal width of 4.6m in $\lambda=75$) at a depth Froude number, F_h , of 0.303 ($F_h = V/\sqrt{gh}$, with $h = 0.32\text{m}$ being the water depth at $\lambda=75$). This figure was adapted from Terziev et al. (2021b) and the results presented therein.

Making use of viscous scaling to partly bypass the expense associated with the availability computational resources can accelerate the routine use of full-scale simulations. More importantly, this could allow researchers and practitioners with access to fewer resources to test novel energy saving devices which are particularly susceptible to scale effects at full-scale Reynolds numbers. Having said so, it is instructive to examine the likely y^+ values one can achieve by maintaining a constant grid while traversing the Reynolds number scale through viscous scaling. This is illustrated in Figure 5 by adding horizontal lines beginning at the highest Δy for each y^+ value given in Figure 3, and extending it throughout the Re range. The horizontal lines demonstrate the y^+ value if the model-scale grid were to be preserved across the Re range. Figure 5 demonstrates that a simulation with an average y^+ of 5 in model scale will result in $y^+ = 30$ for full-scale Reynolds numbers in the case of the KCS. While wall functions are necessary, there is considerably more experience and validation examples of numerical modelling at $y^+ = 30$ than there is at $y^+ = 1000$, or higher.

Regardless of the number of numerical examples demonstrating the efficacy of viscous scaling, validation of local properties with a matching physical experiment is necessary. However, it would likely be difficult to convince a towing facility to fill their tank with a less viscous fluid than water, even if the cost of doing so were to be met. There are also considerations to be made regarding the quantity of fluid necessary, potentially harmful fumes, pollution, and subsequent cleaning. An alternative might to test hulls in wind tunnels (Lee et al., 2003), where the Reynolds numbers are much lower as a result of the properties of air. Laminar-turbulent transition must be handled well by both the experimental facility and CFD solver (where water is used with a modified viscosity instead of air). If these conditions are met and good validation can be achieved, it is possible to argue that viscous scaling should work at full-scales equally as well.

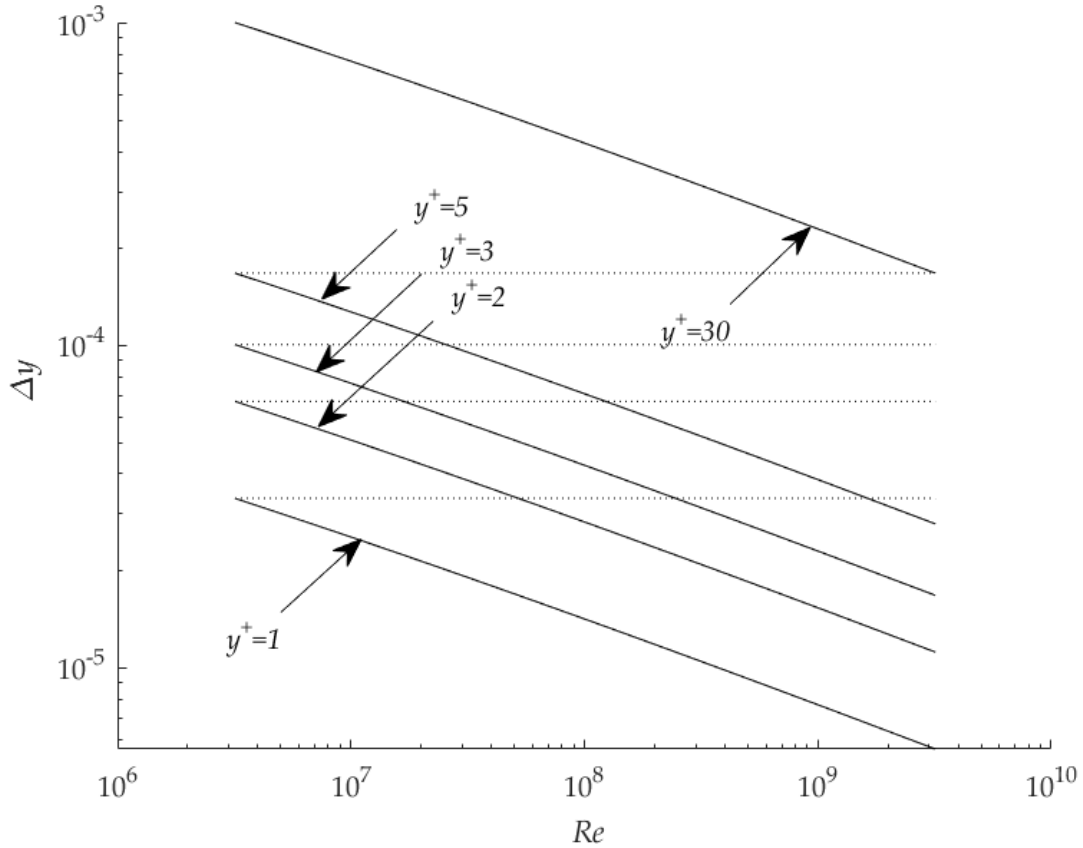


Figure 5. First layer thickness requirements to maintain constant y^+ values of 1, 2, 3, 5, and 30 for Re corresponding to the design speed and scale factors between 1 and 100 for the KCS. These values are computed using Eq. (8). The horizontal lines indicate the result of maintaining a constant near-wall thickness, Δy , while increasing the Re from model to full-scale.

Other evidence may be obtained from towing tanks. For example, Ridgely-Nevitt (1959) showed a difference of 12°F ($\approx 11^\circ\text{C}$) in water temperature caused a significant difference in the resistance curve which was greatest at low Froude numbers. In such cases differences can only be attributed to Reynolds number effects, which are in no way different from viscous scaling. The near-field flow dominates the low F_n contribution to resistance and suffers the greatest scale effects, as demonstrated earlier. While the Reynolds number difference is likely very limited, temperature variations can further open up the potential for experimental viscous scaling examinations.

Another method to achieve full similarity is through the use of polymer additives, explored by Khomyakov and Elyukhina (2019). In this approach, polymer additives are dissolved in the boundary layer. This has the effect of reducing turbulent friction losses by up to 80% (White and Mungal, 2008). The dissolved quantities are in the range of several parts per million in typical applications, but pollution concerns are likely nevertheless. The study of Khomyakov and Elyukhina (2019) used a circulating

flow channel, meaning that no wave effects were present. Therefore, using this approach in a conventional towing tank is desirable to study the effects of polymer additives further.

3.3 Present state and achievements of full-scale ship CFD

Full-scale ship CFD has been practiced for more than two decades. Yet the accuracy of such predictions are not considered robust. Since all energy saving devices either operate within the boundary layer or wake of a vessel, scale effects can have a profound impact on performance. For example, the thickness of the boundary layer can change drastically, as shown in Figure 4. The corollary being that model-scale predictions of an energy saving or wake modifying device operating within the area most affected by viscosity can suffer significant scale effects. Ship owners are justifiably averse to installing and testing novel technologies, since the uncertainties involved are too large at present.

Potential gains from energy saving devices are typically of the same order of magnitude as the uncertainties caused by scale effects (K. Song et al., 2019). Alternatively, where such devices are analysed at full-scale, uncertainties associated with the CFD set-up can be equally problematic, particularly since there are currently no established modelling procedures. This has not discouraged many researchers from studying full-scale ship flows, resulting in a rather sizable body of literature devoted to the topic, even though validation is usually not possible due to the lack of data.

Some recent contributions to full-scale ship hydrodynamic examinations using CFD include Terziev et al. (2021a, 2021b, 2019) where geometrically similar series of the KCS hull are analysed for a variety of conditions. Findings from these studies include the confirmation of scale effects on the form factor, wave resistance coefficient, and the CFD-based detection of a wave component influence on the frictional resistance. To the best of our knowledge, Terziev et al. (2019) is the only study to compare CFD with experimental data at three scale factors for the same Froude number and demonstrate persistently good accuracy. Park et al. (2015) studied the performance of an energy saving device at model and full-scale. They proposed a procedure to study full-scale flows which they claim is reliable and efficient.

Pereira et al. (2017) collected resistance data from other sources and demonstrated an unacceptable spread in predictions. They raised the question of whether such a spread is a consequence of modelling errors, numerical error, or a combination of the two. Pereira et al. (2017) then used 14 turbulence models on between 7 and 9 systematically refined grids at model and full-scale in an attempt to provide an answer. Interestingly, they showed that discretisation uncertainty can be larger or smaller depending on the investigated parameter. For example, their form factor estimates at full-scale were

characterised by higher uncertainty regardless of turbulence model, while the opposite was true for some turbulence models in the case of the wake fraction.

Bhushan et al. (2009) performed model and full-scale simulations of the Athena hull, for which they had access to full-scale data. Their results were validated in the sense that the comparison error was smaller than the validation uncertainty (ITTC, 2017). However, the absolute values of the error and validation uncertainty were in the range of 9% - 12%, which is too high, and demonstrates one of the chief problems with full-scale experimentation – considerable uncertainties. A 0.1% comparison would have little value if the experimental uncertainty is in the range of 10%, which is usually the case. Additionally, as Pereira et al. (2017) point out, visual comparisons are frequently the only measure of accuracy used in comparing wave fields and wakes, which are unreliable. To resolve this situation, international collaborative efforts are necessary to hone in on best practice approaches both experimentally and computationally.

Tahara et al. (2002) investigated the optimum simulation technique for ship viscous flow at full-scale Reynolds number using two-point wall-function method. They highlighted the difficulty in maintaining adequate resolution in the boundary layer

The EFFORT (European Full-scale Flow Research and Technology) project between 2002 and 2005 targeted the development of CFD tools to study full-scale flows (Bugalski, 2007). This project consisted of full-scale measurements, model testing, CFD development, validation and verification, and applications and demonstration. Unfortunately, many of the results obtained during the EFFORT project are at least partly classified or proprietary, limiting their re-use. Nevertheless, this project demonstrated that further research is necessary at the set up and development ends of ship CFD.

3.3.1 The 2016 Lloyd’s Register full-scale ship hydrodynamics workshop

Representatives 15 countries came together in November 2016 with the aim of building confidence in full-scale ship CFD during a workshop organised by Lloyd’s Register (Ponkratov, 2016). This international effort was the first numerical modelling workshop to focus exclusively on full-scale ship hydrodynamics. More importantly, it provided data for validation, which is extremely rare and usually proprietary. This has historically meant that full-scale research is not able to provide validation. For example, recent studies in full-scale ship hydrodynamics use geometries or data that are not accessible to other researchers (Mikkelsen et al., 2019; Sun et al., 2020). In this sense, the Lloyd’s Register data is a potential game changer and the plan of further full-scale trials are particularly welcome.

The Lloyd’s Register report reveals a large spread of results and adopted approaches. For example, some participants did not model the free surface and opted for a double

body method, while others modelled the superstructure and its corresponding wind resistance. Similarly, some modelled sinkage and trim, while others did not. This likely contributes to the relatively large spread in predictions. The results of this report are in a sense similar to the early ship hydrodynamics workshops where model scale results were examined. However, the achievements of some participants, who attained comparison errors within 3% should not be minimised.

One of the participants who achieved high accuracy summarised their work in a white paper on full-scale ship hydrodynamics (Peric, 2019), where it was highlighted that experienced users can provide robust results. Reliance on experience and presently available numerical modelling techniques may be adequate for highly experienced users, but it will not enable a sufficiently rapid transition to routine high-quality full-scale ship CFD. For this reason, increasingly adaptive solvers are necessary. For example, adaptive meshing, time marching and turbulence modelling.

3.3.2 Lessons and outlook from model-scale ship hydrodynamics workshops

The numerical workshops on model-scale ship hydrodynamics can provide some insight into how full-scale workshops might evolve. For example, computational power availability and cell numbers were given earlier as a key bottleneck. It is therefore interesting to examine how submissions to such workshops have changed over time. Figure 6 contains the reported cell numbers in workshops held in the years 2000, 2010, 2015, and 2016; the latter being the full-scale workshop.

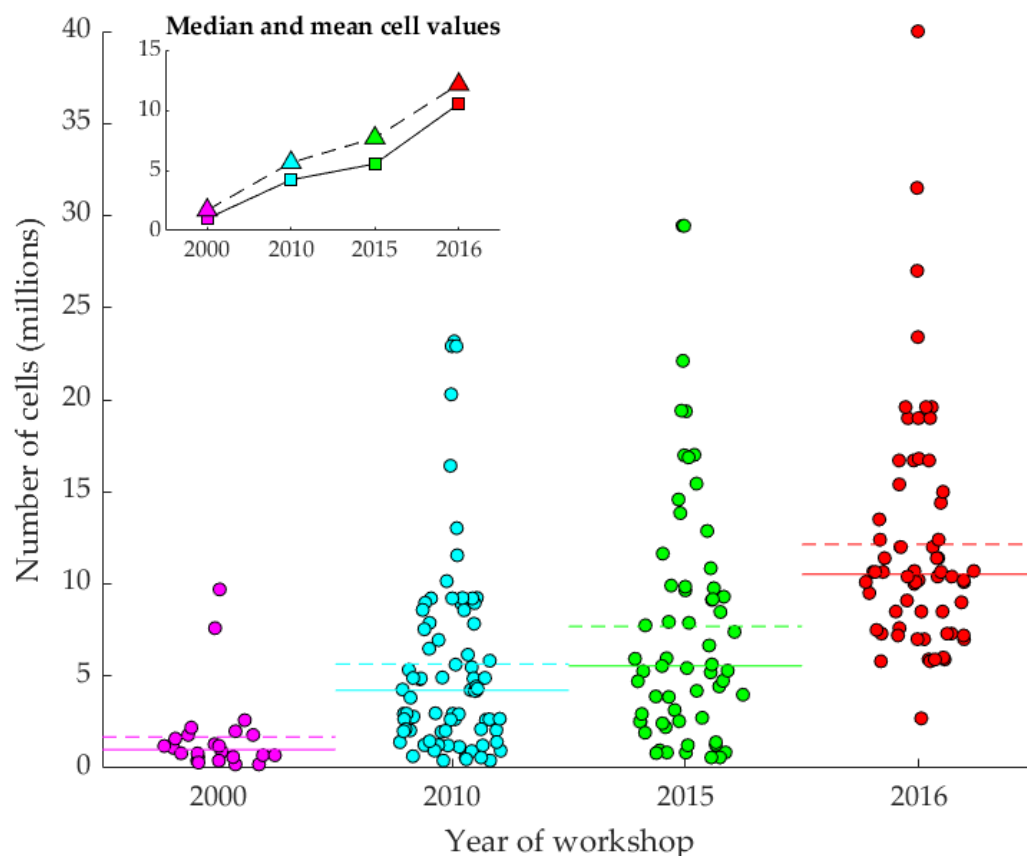


Figure 6. Cell numbers reported in numerical hydrodynamics workshops. Note that some participants' contributions with high numbers cells have been excluded to avoid skewing the vertical axis. These data were collected from Hino et al. (2020), Larsson et al. (2014, 2003), and Ponkratov (2016). In the main plot, solid lines indicate median values, while dashed lines indicate mean values. These are represented by squares and triangles in the small plot, respectively.

Figure 6 shows two important trends. Firstly, the number of participants increased following the first model-scale workshop. This is likely to be replicated with any subsequent full-scale workshop. Secondly, the cell numbers have been increasing rapidly over the past two decades. The focus in Figure 6 should not be the highest cell numbers. There will always be some participants with access to considerably more resources than others, but these are not representative of the general CFD community. It is more important to focus on the mean and median values, which have grown considerably. It is similarly important to consider the data in conjunction with the error against experimental data, where this is available. Figure 7 shows this data for the 2010 and 2015 workshops, where this information is readily available.

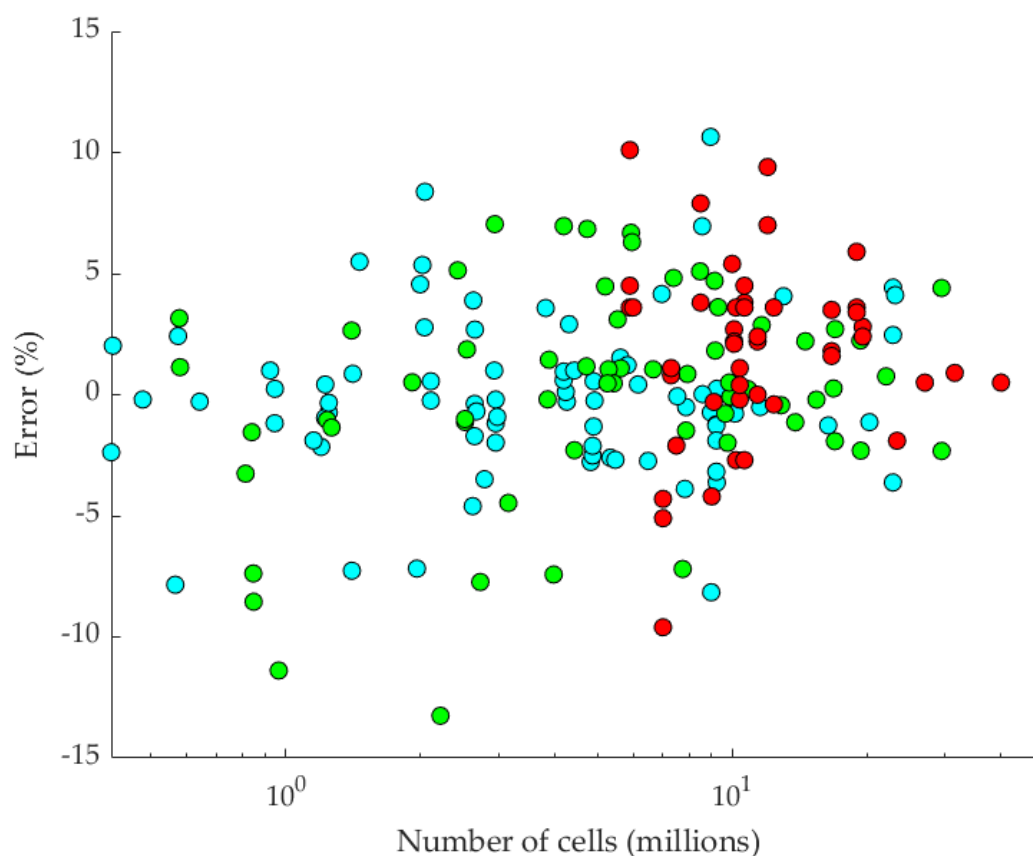


Figure 7. Number of cells and corresponding error for the 2010 (cyan), 2015 (green), and 2016 (red) workshops. This figure was constructed using results found in Hino et al. (2020), Larsson et al. (2014), and Ponkratov (2016). The 2010 and 2015 workshop results are resistance errors, while the 2016 – achieved speed.

In the five-year period between the two workshops, the median and mean error of the predictions changed from -0.29% and -0.66% to 0.5% and 0.13%, respectively. This can also be confirmed by visual inspection of Figure 7: the scatter along the vertical axis has not changed noticeably despite the increase in cell numbers. Moreover, cell numbers in the region of 1-2 million cells are frequently more accurate than predictions with much higher cell numbers. To solidify this conclusion, more numerical simulations are necessary with more than 20 million cells. This is necessary, because the standard deviation of the error rose from 3.29% to 4.31% from 2010 to 2015, indicating a problematic trend – higher cell numbers on average resulted in a higher spread of the error. It should also be noted that experimental uncertainties are estimated in the range of 1%, i.e. these cannot explain the observed disagreements.

On the other hand, the full-scale results show a marked overprediction bias, with 72% of results having a positive error (36 out of 50 results). The mean and median errors for this workshop are 2.3% and 1.9%, respectively with a standard deviation of 3.6%. While these results may suggest that the full-scale predictions have a lesser spread than the 2015 model-scale workshop, such a conclusion would be premature. The

depicted results from the full-scale workshop take into account the speed achieved by the vessel for a given propeller rotation rate. Depending on the propeller rotation rate, the participants' spread in results can be greater.

The scatter evident in Figure 7 suggests that resistance prediction even at model scale remains a non-trivial problem. It may therefore be too early to claim that high-quality CFD can be produced routinely. Rather, further standardisation is required. This conclusion will likely apply to any future full-scale workshops, but it is hoped that with time, average spread and accuracy of results can be improved.

4. Conclusions

It is difficult to overstate the value of robust full-scale ship resistance predictions. Achieving routine, high-quality numerical simulation at large Reynolds numbers will enable advances in energy efficiency and help ship owners or operators meet increasingly strict local and international standards. A prerequisite to this is the sufficient reduction of uncertainties to demonstrate the efficacy of energy saving devices in validated, full-scale operational conditions.

Additionally, once full-scale ship CFD becomes more established, the field of ship hydrodynamics will move on from tolerating and correcting for scale effects. Some of the key conditions necessary to enable this transition include the increased availability of computational power and the implementation of increasingly adaptive numerical set-ups to unlock CFD for a greater number of users. However, the most critical condition is the availability of openly available high-quality datasets for validation purposes. This is the main bottleneck at present, and if not resolved, it will continue to restrict confidence in full-scale simulation with knock-on effects on innovation and energy efficiency achievements.

Many decades have passed since scale effects were identified and research began attempting to devise corrections for them. These decades have not produced unified and universally applicable equations. It is important to remember that model-scale results give nothing more than the results for a model ship. There is currently no satisfactory extrapolation method that bypasses all scale effects and works for different hulls. The methods currently in use were designed to be short term solutions many decades ago. While the field has advanced and moved on from many of the concerns and problems of that time, there is still no unified formula that all researchers can agree represents the frictional resistance of a flat plate or ship, particularly at full-scale Reynolds numbers.

We do not believe the problems of extrapolation procedures can be reconciled with the physics of ship resistance scaling, and while extrapolation procedures are highly successful, there will be a time where they are no longer necessary. The goal of the

research community should be to accelerate this transition. Efforts must be directed towards establishing standards in full-scale simulation practice and accruing openly available full-scale data. The acid test of whether extrapolation procedures remain necessary is the spread and accuracy of CFD predictions at model and full-scale. At present, it appears this test is not met, as demonstrated in section 3.3.2.

In the course of this review, several items were recommended for future research. These can be summarised and supplemented as follows. Further research is necessary to determine the nature of the scale effect of the form factor. While the extrapolation procedure itself (2D or 3D) cannot account for all physical phenomena, its utility will persist until such a time as full-scale simulation becomes sufficiently reliable. Research on scale effects in the interim is therefore necessary. For example, it would be interesting to settle the disagreement between Ferguson (1977) and Yokoo (1960) regarding sinkage and trim, explored in section 2.2.1.2. This would help progress the debate around scale effects on sinkage and trim which will find applications in shallow waters as well as in general cases. Moreover, this can improve the understanding of factors influencing ship sinkage and trim, possibly leading to improved predictions and design.

Accurate transition modelling is a crucial factor for low Froude number ship hydrodynamics. Further research and guidance on modelling practices is necessary. Most turbulence models are known to be capable of exhibiting transition properties (Eca and Hoekstra, 2008), but to the best of our knowledge, no guidelines exist for their application on ships. It is possible to incorporate an intermittency transport equation to model transition, use low wall-distance-based Re damping modifications, or suppress turbulence within a predefined region depending on the turbulence model. Our experience suggests that the addition of transition through a transport equation is not necessarily beneficial when using a general set up (Terziev et al., 2020). The problem of transition, which typically requires $y^+ < 1$, and its modelling at full-scale is also likely to be a challenging problem because of the near-wall grid-related challenges explored in section 3.1.2.1.

There are several areas we did not explore in detail in this paper. Specifically, roughness effects were discussed from the point of view of turbulence only, deferring a full description to (Andersson et al., 2020). Scale effects act on propellers in ways this review did not explore, for example, cavitation and noise, as explained by Sánchez-Caja et al. (2014) and Yao and Zhang (2018).

Very high y^+ modelling of full-scale flows ($y^+ > 1,000$) must be demonstrated by more researchers to increase confidence in the approach. Similarly, viscous scaling should be explored as a promising strategy to bypass the excessive grid requirements of high Reynolds number flows. Ideally, this would be accompanied by creative experiments

and validation strategies. Shallow and confined water scale effects, particularly when clearances between a hull and the canal or seabed are small are of also particular interest due to important role viscosity plays.

Acknowledgements

The authors are grateful to the International Conference on Postgraduate Research in Maritime Technology 2021 (PostGradMarTec 2021) organised by the Confederation of European Maritime Technology Societies for allowing the presentation of a short version of this paper entitled '*A short review of scale effects in ship hydrodynamics with emphasis on CFD applications*' between 3rd – 4th November 2021. The full text of the short version of this paper may be accessed via the University of Strathclyde repository, Pure, using the following link: <https://pureportal.strath.ac.uk/en/publications/a-short-review-of-scale-effects-in-ship-hydrodynamics-with-emphas>

References

- Andersson, J., Oliveira, D.R., Yeginbayeva, I., Leer-Andersen, M., Bensow, R.E., 2020. Review and comparison of methods to model ship hull roughness. *Appl. Ocean Res.* 99, 102119. <https://doi.org/10.1016/j.apor.2020.102119>
- Baar, J., Price, W., 1988. Developments in the Calculation of the Wavemaking Resistance of Ships. *Proc. R. Soc. Lond. A. Math. Phys. Sci.* 416, 115–147.
- Baba, E., 1966. A new component of viscous resistance of ships. *J. Soc. Nav. Archit. Japan* 44, 23–34. <https://doi.org/10.1016/b978-0-12-021803-5.50007-4>
- Beck, R.F., 1971. Wave resistance of a thin ship with a rotational wake. *J. Sh. Res.* 15, 196–216.
- Bhushan, S., Xing, T., Carrica, P., Stern, F., 2009. Model- and Full-Scale URANS Simulations of Athena Resistance, Powering, Seakeeping, and 5415 Maneuvering. *J. Sh. Res.* 53, 179–198.
- Brard, R., 1970. Viscosity, Wake, and Ship Waves. *J. Sh. Res.* 14, 1–34.
- Bugalski, T., 2007. An overview of the selected results of the European Union Project EFFORT. *Arch. Civ. Mech. Eng.* 7, 55–67. [https://doi.org/10.1016/S1644-9665\(12\)60013-2](https://doi.org/10.1016/S1644-9665(12)60013-2)
- Chow, S.-K., 1967. Free-Surface Effects on Boundary-Layer Separation on Vertical Struts.
- Dand, W.I., 1967. The wavemaking resistance of ships: Vertical force and form resistance of a hull at uniform velocity. PhD Thesis. University of Glasgow.
- Date, C.J., Turnock, S., 1999. A study into the techniques needed to accurately predict a skin friction using RANS solvers with validation against Froude's historical flat plate experimental data, Ship science report No. 114.
- De Rouck, J., Geeraerts, J., Troch, P., Kortenhaus, A., Pullen, T., Franco, L., 2005. New results on scale effects for wave overtopping at coastal structures, in: *Proceedings of the International Conference on Coastlines, Structures and Breakwaters*. pp. 29–43.
- Demirel, Y.K., Khorasanchi, M., Turan, O., Incecik, A., Schultz, M.P., 2014. A CFD model for the frictional resistance prediction of antifouling coatings. *Ocean Eng.* 89, 21–31. <https://doi.org/10.1016/j.oceaneng.2014.07.017>
- Demirel, Y.K., Turan, O., Incecik, A., 2017. Predicting the effect of biofouling on ship resistance using CFD. *Appl. Ocean Res.* 62, 100–118. <https://doi.org/10.1016/j.apor.2016.12.003>
- Duffal, V., De Laage de Meux, B., Manceau, R., 2019. Development and validation of a hybrid RANS-LES approach based on temporal filtering. *ASME-JSME-KSME*

- 2019 8th Jt. Fluids Eng. Conf. AJKFluids 2019 2, 1–10.
<https://doi.org/10.1115/AJKFluids2019-4937>
- Durbin, P.A., Pettersson Reif, B.A., 2011. Statistical theory and modelling for turbulent flow, Second Edi. ed. Wiley.
- Eca, L., Hoekstra, M., 2011. On the application of wall functions in ship viscous flows. Mar. 2011 - Comput. Methods Mar. Eng. IV 585–604.
- Eca, L., Hoekstra, M., 2008. The numerical friction line. J. Mar. Sci. Technol. 13, 328–345. <https://doi.org/10.1007/s00773-008-0018-1>
- Elsherbiny, K., Tezdogan, T., Kotb, M., Incecik, A., Day, S., 2019. Experimental analysis of the squat of ships advancing through the New Suez Canal. Ocean Eng. 178, 331–344. <https://doi.org/10.1016/j.oceaneng.2019.02.078>
- Fadai-Ghotbi, A., Friess, C., Manceau, R., Gatski, T.B., Borée, J., 2010. Temporal filtering: A consistent formalism for seamless hybrid RANS-LES modeling in inhomogeneous turbulence. Int. J. Heat Fluid Flow 31, 378–389.
<https://doi.org/10.1016/j.ijheatfluidflow.2009.12.008>
- Ferguson, A.M., 1977. Factors affecting the components of ship resistance. PhD Thesis. University of Glasgow.
- Gadd, G.E., 1967. A new turbulent friction formulation based on a reappraisal of Hughes' results. Trans. RINA 109, 109–511.
- García-Gómez, A., 2000. On the form factor scale effect. Ocean Eng. 27, 97–109.
[https://doi.org/10.1016/S0029-8018\(98\)00042-0](https://doi.org/10.1016/S0029-8018(98)00042-0)
- Girimaji, S.S., Abdol-Hamid, K.S., 2005. Partially-averaged navier stokes model for turbulence: Implementation and validation, in: 43rd AIAA Aerospace Sciences Meeting and Exhibit - Meeting Papers, Reno, Nevada. pp. 1–14.
<https://doi.org/10.2514/6.2005-502>
- Gotman, A., 2020. Residual resistance of displacement vessels. J. Mar. Sci. Eng. 8.
<https://doi.org/10.3390/JMSE8060400>
- Gotman, A., 2002. Study Of Michell's Integral And Influence Of Viscosity And Ship Hull Form On Wave Resistance. Ocean. Eng. Int. 6, 74–115.
- Grigson, C.W.B., 1999. A planar friction algorithm and its use in analysing hull resistance. Trans. RINA.
- Haase, M., Davidson, G., Binns, J., Thomas, G., Bose, N., 2016a. Full-scale resistance prediction in finite waters: A study using computational fluid dynamics simulations, model test experiments and sea trial measurements. Proc. Inst. Mech. Eng. Part M J. Eng. Marit. Environ. 231, 316–328.
<https://doi.org/10.1177/1475090216642467>

- Haase, M., Zurcher, K., Davidson, G., Binns, J.R., Thomas, G., Bose, N., 2016b. Novel CFD-based full-scale resistance prediction for large medium-speed catamarans. *Ocean Eng.* 111, 198–208. <https://doi.org/10.1016/j.oceaneng.2015.10.018>
- Heller, V., 2011. Scale effects in physical hydraulic engineering models. *J. Hydraul. Res.* 49, 293–306. <https://doi.org/10.1080/00221686.2011.578914>
- Hino, T., Stern, F., Larsson, L., Visonneau, M., Hirakata, N., Kim, J., 2020. Numerical Ship Hydrodynamics: An Assessment of the Tokyo 2015 Workshop.
- Hirt, C. W., Nichols, B. D., 1981. Volume of fluid (VOF) method for the dynamics of free boundaries. *J. Comput. Phys.* 39, 201–225. [https://doi.org/10.1016/0021-9991\(81\)90145-5](https://doi.org/10.1016/0021-9991(81)90145-5)
- Hughes, G., 1954. Friction and form resistance in turbulent flow and a proposed formulation for use in model and ship correlation. *Trans. Inst. Nav. Arch.* 96.
- ITTC, 2017. Quality System Manual Recommended Procedures and Guidelines Procedure Uncertainty Analysis in CFD Verification and Validation.
- ITTC, 1999. Final Report of the Resistance Committee and Recommendations to the 22nd IITC.
- Katsui, T., Asai, H., Himeno, Y., Tahara, Y., 2005. The proposal of a new friction line, in: Fifth Osaka Colloquium on Advanced CFD Applications to Ship Flow and Hull Form Design, Osaka, Japan.
- Khomyakov, A., Elyukhina, I., 2019. Complete dynamic similarity for sea trials and towing tank experiments by means of polymer drag reduction. *Ocean Eng.* 178, 31–37. <https://doi.org/10.1016/j.oceaneng.2019.02.061>
- Kok, Z., Duffy, J., Chai, S., Jin, Y., Javanmardi, M., 2020. Numerical investigation of scale effect in self-propelled container ship squat. *Appl. Ocean Res.* 99. <https://doi.org/10.1016/j.apor.2020.102143>
- Korkmaz, K.B., Werner, S., Bensow, R.E., 2019. Numerical friction lines for CFD based form factor determination, in: VIII International Conference on Computational Methods in Marine Engineering MARINE 2019.
- Korkmaz, K.B., Werner, S., Sakamoto, N., Queutey, P., Deng, G., Yuling, G., Guoxiang, D., Maki, K., Ye, H., Akinturk, A., Sayeed, T., Hino, T., Zhao, F., Tezdogan, T., Demirel, Y.K., Bensow, R., 2021. CFD based form factor determination method. *Ocean Eng.* 220, 108451. <https://doi.org/10.1016/j.oceaneng.2020.108451>
- Landweber, L., Patel, V.C., 1979. Ship Boundary Layers. *Annu. Rev. Fluid Mech.* 11, 173–205. <https://doi.org/10.1146/annurev.fl.11.010179.001133>
- Lap, A.J.W., 1956. The frictional drag of smooth ship forms. *Int. Shipbuild. Prog.* 3,

- 573–587. <https://doi.org/10.3233/isp-1956-32702>
- Larsson, L., Stern, F., Bertram, V., Bertrami, V., 2003. Benchmarking of Computational Fluid Dynamics for Ship flows: The Gothenburg 2000 Workshop. *J. Sh. Res.* 47, 63–81.
- Larsson, L., Stern, F., Visonneau, M., 2014. *Numerical Ship Hydrodynamics: An assessment of the Gothenburg 2010 Workshop*. Springer. <https://doi.org/10.1007/978-94-007-7189-5>
- Lazauskas, L. V., 2009. *Resistance, Wave-Making and Wave-Decay of Thin Ships, with Emphasis on the Effects of Viscosity*.
- Lee, M., Moser, R.D., 2015. Direct numerical simulation of turbulent channel flow up to $Re\tau \approx 5200$. *J. Fluid Mech.* 774, 395–415. <https://doi.org/10.1017/jfm.2015.268>
- Lee, S.J., Kim, H.R., Kim, W.J., Van, S.H., 2003. Wind tunnel tests on flow characteristics of the KRISO 3,600 TEU containership and 300K VLCC double-deck ship models. *J. Sh. Res.* 47, 24–38.
- Liefvendahl, M., Fureby, C., 2017. Grid requirements for LES of ship hydrodynamics in model and full scale. *Ocean Eng.* 143, 259–268. <https://doi.org/10.1016/j.oceaneng.2017.07.055>
- Manceau, R., 2019. Hybrid temporal LES: Development and applications, ERCOFTAC Bulletin, European Research Community on Flow, Turbulence and Combustion, 2019, Progress in RANS-based Scale-Resolving Flow Simulation Methods.
- Maynord, S.T., 2006. Evaluation of the Micromodel: An Extremely Small-Scale Movable Bed Model. *J. Hydraul. Eng.* 132, 343–353. [https://doi.org/10.1061/\(ASCE\)0733-9429\(2006\)132](https://doi.org/10.1061/(ASCE)0733-9429(2006)132)
- McNaughton, K.G., Brunet, Y., 2002. Townsend’s Hypothesis, Coherent Structures And Monin–Obukhov Similarity. *Boundary-Layer Meteorology. Boundary-Layer Meteorol.* 102, 161–175.
- Michell, J.H., 1898. The wave-resistance of a ship. London, Edinburgh, Dublin *Philos. Mag. J. Sci.* 45, 106–123.
- Mikkelsen, H., Steffensen, M.L., Ciortan, C., Walther, J.H., 2019. Ship scale validation of CFD model of self-propelled ship. *Mar. 2019 Comput. Methods Mar. Eng.* VIII 718–729.
- Min, K.-S., Kang, S.-H., 2010. Study on the form factor and full-scale ship resistance. *J. Mar. Sci. Technol.* 15, 108–118. <https://doi.org/10.1007/s00773-009-0077-y>
- Molland, A.F., Turnock, S.R., Hudson, D.A., 2017. Components of Hull Resistance, in: *Ship Resistance and Propulsion: Practical Estimation of Ship Propulsive*

- Power. Cambridge University Press, Cambridge, pp. 12–69.
<https://doi.org/10.1017/9781316494196.005>
- Nisham, A., Terziev, M., Tezdogan, T., Beard, T., Incecik, A., 2021. Prediction of the aerodynamic behaviour of a full-scale naval ship in head waves using Detached Eddy Simulation. *Ocean Eng.* 222, 108583.
<https://doi.org/10.1016/j.oceaneng.2021.108583>
- Park, D.W., 2015. A study on the effect of flat plate friction resistance on speed performance prediction of full scale. *Int. J. Nav. Archit. Ocean Eng.* 7, 195–211.
<https://doi.org/10.2478/IJNAOE-2015-0014>
- Park, S., Oh, G., Hyung Rhee, S., Koo, B.Y., Lee, H., 2015. Full scale wake prediction of an energy saving device by using computational fluid dynamics. *Ocean Eng.* 101, 254–263. <https://doi.org/10.1016/j.oceaneng.2015.04.005>
- Pena, B., Muk-Pavic, E., Ponkratov, D., 2019. Achieving a high accuracy numerical simulations of the flow around a full scale ship, in: *Proceedings of the International Conference on Offshore Mechanics and Arctic Engineering - OMAE*. pp. 1–10. <https://doi.org/10.1115/OMAE2019-95769>
- Pereira, F.S., Eca, L., Vaz, G., 2017. Verification and Validation exercises for the flow around the KVLCC2 tanker at model and full-scale Reynolds numbers. *Ocean Eng.* 129, 133–148. <https://doi.org/10.1016/j.oceaneng.2016.11.005>
- Peric, M., 2019. White paper: Full-scale simulation for marine design. Siemens White Pap.
- Ponkratov, D., 2016. Lloyd's Register workshop on ship scale hydrodynamics, in: Ponkratov, D. (Ed.), *2016 Workshop on Ship Scale Hydrodynamic Computer Simulation*. p. 2016. <https://doi.org/10.1002/ejoc.201200111>
- Prandtl, L., 1925. Report on the investigation of developed turbulence, Translation of "Bericht über Untersuchungen zur ausgebildeten Turbulenz." *Zeitschrift für angewandte Mathematik und Mechanik*, vol. 5, no. 2, April 1925.
- Ridgely-Nevitt, C., 1959. Geometrically similar models. *Int. Shipbuild. Prog.* 6, 311–339. <https://doi.org/10.3233/isp-1959-65903>
- Runchal, A., 2020. 50 Years of CFD in Engineering Sciences, 50 Years of CFD in Engineering Sciences. <https://doi.org/10.1007/978-981-15-2670-1>
- Sánchez-Caja, A., González-Adalid, J., Pérez-Sobrino, M., Sipilä, T., 2014. Scale effects on tip loaded propeller performance using a RANSE solver. *Ocean Eng.* 88, 607–617. <https://doi.org/10.1016/j.oceaneng.2014.04.029>
- Schlichting, H., 1979. *Boundary-Layer Theory*, 7th ed. McGraw-Hill.
<https://doi.org/10.1007/978-3-662-52919-5>

- Schoenherr, K., 1932. Resistance of flat surfaces moving through a fluid. *Trans. Soc. Nav. Arch. Mar. Eng.* 40, 279–313.
- Schultz-Grunow, F., 1941. New frictional resistance law for smooth plates.
- Sezen, S., Cakici, F., 2019. Numerical Prediction of Total Resistance Using Full Similarity Technique. *China Ocean Eng.* 33, 493–502.
<https://doi.org/10.1007/s13344-019-0047-z>
- Shevchuk, I., Böttner, C.U., Kornev, N., 2016. Numerical Analysis of the Flow in the Gap Between the Ship Hull and the Fairway Bottom in Extremely Shallow Water. *Proc. 4th Int. Conf. Sh. Manoeuvring Shallow Confin. Water (MASHCON)*, 23 - 25 May 2016, Hamburg, Ger. 0, 37–42.
<https://doi.org/10.18451/978-3-939230-38-0>
- Shivachev, E., Khorasanchi, M., Day, A.H., 2017. Trim influence on KRISO container ship (KCS); an experimental and numerical study, in: *Proceedings of the ASME 2017 36th International Conference on Ocean, Offshore and Arctic Engineering*. pp. 1–7. <https://doi.org/10.1115/OMAE2017-61860>
- Simonsen, C.D., Otzen, J.F., Joncquez, S., Stern, F., 2013. EFD and CFD for KCS heaving and pitching in regular head waves. *J. Mar. Sci. Technol.* 18, 435–459.
<https://doi.org/10.1007/s00773-013-0219-0>
- Song, K., Guo, C., Wang, C., Sun, C., Li, P., Zhong, R., 2019. Experimental and numerical study on the scale effect of stern flap on ship resistance and flow field. *Ships Offshore Struct.* 0, 1–17.
<https://doi.org/10.1080/17445302.2019.1697091>
- Song, S., Demirel, Y.K., Atlar, M., 2019. An investigation into the effect of biofouling on the ship hydrodynamic characteristics using CFD. *Ocean Eng.* 175, 122–137.
<https://doi.org/10.1016/j.oceaneng.2019.01.056>
- Spalart, R., 2001. *Young-Person's Guide Simulation Grids Detached-Eddy*.
- Sun, W., Hu, Q., Hu, S., Su, J., Xu, J., Wei, J., 2020. Numerical Analysis of Full-Scale Ship Self-Propulsion Performance with Direct Comparison to Statistical Sea Trial Results. *J. Mar. Sci. Eng.* 8, 1–22.
- Tahara, Y., Katsui, T., Himeno, Y., 2002. Computation of Ship Viscous Flow at Full Scale Reynolds Number. *J. Soc. Nav. Archit. Japan* 92, 89–101.
- Tatinclaux, B.J., 1970. Effect of a Rotational Wake on the Wavemaking Resistance of an Ogive. *J. Sh. Res.* 14, 84–99.
- Telfer, E. V., 1927. Ship resistance similarity. *Trans. R. Inst. Nav. Archit.* 69, 174–190.
- Terziev, M., Tezdogan, T., Demirel, Y.K., Villa, D., Mizzi, S., Incecik, A., 2021a. Exploring the effects of speed and scale on a ship's form factor using CFD. *Int. J.*

- Nav. Archit. Ocean Eng. 13, 147–162. <https://doi.org/10.1016/j.ijnaoe.2020.12.002>
- Terziev, M., Tezdogan, T., Incecik, A., 2021b. A numerical assessment of the scale effects of a ship advancing through restricted waters. *Ocean Eng.* 229, 108972. <https://doi.org/10.1016/j.oceaneng.2021.108972>
- Terziev, M., Tezdogan, T., Incecik, A., 2020. Application of eddy-viscosity turbulence models to problems in ship hydrodynamics. *Ships Offshore Struct.* 15. <https://doi.org/10.1080/17445302.2019.1661625>
- Terziev, M., Tezdogan, T., Incecik, A., 2019. A geosim analysis of ship resistance decomposition and scale effects with the aid of CFD. *Appl. Ocean Res.* 92. <https://doi.org/10.1016/j.apor.2019.101930>
- Todd, F., 1965. The Model-Ship Correlation Problem.
- Tuck, E.O., 1978. Hydrodynamic Problems of Ships in Restricted Waters. *Annu. Rev. Fluid Mech.* 10, 33–46.
- Varghese, J., Durbin, P.A., 2020. Representing surface roughness in eddy resolving simulation. *J. Fluid Mech.* 897. <https://doi.org/10.1017/jfm.2020.368>
- Vaz, G., Eca, L., Pereira, F.S., 2017. On the Prediction of Shear-Layer Flows With Rans and SRS Models, in: VII International Conference on Computational Methods in Marine Engineering MARINE 2017 M. Visonneau, P. Queutey and D. Le Touz'e (Eds) ON. pp. 1–17. <https://doi.org/10.1016/j.compfluid.2016.05.031>
- Wackers, J., Koren, B., Raven, H.C., van der Ploeg, A., Starke, A.R., Deng, G.B., Queutey, P., Visonneau, M., Hino, T., Ohashi, K., 2011. Free-Surface Viscous Flow Solution Methods for Ship Hydrodynamics. *Arch. Comput. Methods Eng.* 18, 1–41. <https://doi.org/10.1007/s11831-011-9059-4>
- Wang, Z.J., Chi, X.K., Shih, T., Bons, J., 2004. Direct simulation of surface roughness effects with RANS and DES approaches on viscous adaptive cartesian grids, in: 34th AIAA Fluid Dynamics Conference and Exhibit. pp. 1–12. <https://doi.org/10.2514/6.2004-2420>
- Wang, Z.Z., Xiong, Y., Shi, L.P., Liu, Z.H., 2015. A numerical flat plate friction line and its application. *J. Hydrodyn.* 27, 383–393. [https://doi.org/10.1016/S1001-6058\(15\)60496-6](https://doi.org/10.1016/S1001-6058(15)60496-6)
- White, C.M., Mungal, M.G., 2008. Mechanics and prediction of turbulent drag reduction with polymer additives. *Annu. Rev. Fluid Mech.* 40, 235–256. <https://doi.org/10.1146/annurev.fluid.40.111406.102156>
- White, F., 2010. *Fluid Mechanics*. McGraw-Hill, New York 862. <https://doi.org/10.1111/j.1549-8719.2009.00016.x>. *Mechanobiology*
- White, F., 2006. *Viscous fluid flow*, 3rd ed. McGraw-Hill.

- Wigley, C., 1965. *The Collected Papers of Sir Thomas Havelock on Hydrodynamics*.
- Wilcox, D.C., 2006. *Turbulence modeling for CFD*, 3rd ed, Transportation Research Record. DCW Industries. <https://doi.org/10.1016/j.aqpro.2013.07.003>
- Yao, H., Zhang, H., 2018. Numerical simulation of boundary-layer transition flow of a model propeller and the full-scale propeller for studying scale effects. *J. Mar. Sci. Technol.* 23, 1004–1018. <https://doi.org/10.1007/s00773-018-0528-4>
- Yokoo, K., 1960. Effect of Sinkage and Trim on Form Factor of Resistance. *J. Zosen Kiokai* 15–22. https://doi.org/10.2534/jjasnaoe1952.1960.108_15
- Youden, W.J., 1972. Graphical diagnosis of inter-laboratory test results. *J. Qual. Technol.* 4. <https://doi.org/https://doi.org/10.1080/00224065.1972.11980509>
- Zeng, Q., Hekkenberg, R., Thill, C., 2019. On the viscous resistance of ships sailing in shallow water. *Ocean Eng.* 190, 106434. <https://doi.org/10.1016/j.oceaneng.2019.106434>
- Zhang, J., Minelli, G., Rao, A., Basara, B., Bensow, R., Krajnović, S., 2018. Comparison of PANS and LES of the flow past a generic ship. *Ocean Eng.* 165, 221–236. <https://doi.org/10.1016/j.oceaneng.2018.07.023>
- Zhang, Z.J., Stern, F., 1996. Free-Surface Wave-Induced Separation. *J. Fluids Eng.* 118, 546–554.
- Zhao, D.G., Wang, Y.W., Zhou, G.L., 2020. Uncertainty analysis of ship model resistance test in actual seas. *Brodogradnja* 71, 81–94. <https://doi.org/10.21278/brod71406>